LA-UR-08-5488

Approved for public release; distribution is unlimited.

Title:	Adaptive Evolution of Simian Immunodeficiency Viruses Isolated From Two Conventional Progressor Macaques with NeuroAIDS
Author(s):	B.T. Foley, Z # 097029, T-10/T-Division B.T. Korber, Z # 108817, T-10/T-Divison
Intended for:	Journal: Journal of Infectious Diseases

Los Alamos
NATIONAL LABORATORY
EST. 1943

Form 836 (7/06)

Adaptive Evolution of Simian Immunodeficiency Viruses Isolated From Two Conventional Progressor Macaques with NeuroAIDS

Que Dang,[1] Robert M. Goeken,[1] Charles R. Brown,[1] Ronald Plishka,[1] Alicia Buckler-White,[1] Russell Byrum,[2] Brian T. Foley,[3] Bette T. Korber,[3] and Vanessa M. Hirsch[1,*]

Laboratory of Molecular Microbiology, National Institute of Allergy and Infectious Diseases, National Institutes of Health, Bethesda, Maryland 20892[1]; Bioqual, Inc., Rockville, Maryland, 20850; and Theoretical Biology and Biophysics, Group T-10, Los Alamos National Laboratory, Los Alamos, New Mexico 87545[3]

Running Title: Preferential cell tropism of SIV isolated from CNS

[*] Corresponding author.
LMM, NIAID, NIH
Building 4, Room B1-41
4 Center Drive
Bethesda, MD 20892
Phone: (301) 496-0559
Fax: (301) 480-3129
Email: vhirsch@niaid.nih.gov

ABSTRACT

Simian immunodeficiency virus infection of macaques may result in neuroAIDS, a feature more commonly observed in macaques with rapid progressive disease than in those with conventional disease. This is the first report of two conventional progressors (H631 and H636) with encephalitis in rhesus macaques inoculated with a derivative of SIVsmE543-3. Phylogenetic analyses of viruses isolated from the cerebral spinal fluid (CSF) and plasma from both animals demonstrated tissue compartmentalization. Additionally, virus from the central nervous system (CNS) was able to infect primary macaque monocyte-derived macrophages more efficiently than virus from plasma. Conversely, virus isolated from plasma was able to replicate better in peripheral blood mononuclear cells than virus from CNS. We speculate that these viruses were under different selective pressures in their separate compartments. Furthermore, these viruses appear to have undergone adaptive evolution to preferentially replicate in their respective cell targets. Analysis of the number of potential N-linked glycosylation sites (PNGS) in gp160 showed that there was a statistically significant loss of PNGS in viruses isolated from CNS in both macaques compared to SIVsmE543-3. Moreover, virus isolated from the brain in H631, had statistically significant loss of PNGS compared to virus isolated from CSF and plasma of the same animal. It is possible that the brain isolate may have adapted to decrease the number of PNGS given that humoral immune selection pressure is less likely to be encountered in the brain. These viruses provide a relevant model to study the adaptations required for SIV to induce encephalitis.

INTRODUCTION

Human immunodeficiency virus type 1 (HIV-1) has been shown to invade the central nervous system (CNS) early after systemic infection (30, 66) and neurological complications caused or contributed by HIV-1 infection have been observed in patients with acquired immunodeficiency syndrome (AIDS) (67). A few examples of these disorders are encephalitis, HIV-associated cognitive-motor disorder, cerebral toxoplasmosis, cryptococcal meningitis, vacuolar myelopathy, peripheral neuropathy, and lymphomas (44, 67). The introduction of highly active antiretroviral therapy (HAART) in 1996 has decreased the occurrence of many of these neurologic diseases including HIV-associated dementia (HAD) (63). However, despite the initial success of HAART, the incidence rate as well as the prevalence of HAD has actually risen again due to the increase in the number of people living with HIV/AIDS and the prolonged life span of these individuals (43). Clinically, HAD or AIDS dementia complex (ADC), is defined by the impairment of cognitive, behavioral, and motor function (1, 49) and can vary in severity from a mild, minor cognitive motor disorder to frank dementia with the difference being the degree of impairment to which daily life is affected (1). Major neuropathological features characterizing HIV-1 infection in the brain are microglial nodules, reactive astrocytes, perivascular infiltrates, white matter pallor (48), and the presence of syncytia or multinucleated giant cells (MGNC) consisting of macrophages (16, 48, 59). This latter feature is considered the hallmark of HIV encephalitis (HIVE) (65). In addition, perivascular cuffing, the accumulation of perivascular macrophages around blood vessels is also observed (48). The presence of HIVE is consistent with the diagnosis of ADC (1, 8, 48). Interestingly, despite the invasion of HIV-1 in the brain

during primary infection, ADC is generally not observed until much later, when the patient has progressed to AIDS (58, 69).

Simian immunodeficiency viruses (SIV) are nonhuman primate lentiviruses that are closely related to HIV-1 and human immunodeficiency virus type 2 (HIV-2) in that they have similar genomic organization, morphology, and biologic properties (9, 22, 42). Like HIV infection in humans, SIV can cause AIDS in macaques (41) with symptoms of wasting, decline in $CD4^+$ T cells, opportunistic infections, lymphomas, cognitive and motor impairments, and encephalitis. The survival time for the majority of SIV-infected macaques that develop AIDS range from one to three years (11, 28) in comparison to the ten years or more in humans (55); however, a small percentage of infected animals will develop a rapid disease progression with death occurring by approximately three to six months (28). This shortened survival time of rapid progressor (RP) animals has been correlated with the presence of SIV-induced encephalitis (SIVE) (3, 70). Histopathological changes in the brain such as multinucleated giant cells, microglial nodules, and perivascular infiltrates identical to those seen in humans with HIVE, have also been observed in macaques with encephalitis (60, 64). Indeed, SIV neuropathogenesis can recapitulate key elements of HIV-1 neuropathogenesis (40). Therefore, the SIV-infected macaque is an excellent animal model to study the pathogenesis of HIV-associated encephalitis (60, 64).

SIV neuropathogenesis has been shown to occur in both rhesus and pig-tailed macaques inoculated with SIVmac251, SIVmac239, SIV Delta B670/SIV17E-Fr, SIVmac182, and SIVsmFGb (5, 34, 51, 52, 61, 62, 70, 74). In these studies, the

89 percentage of animals observed with a rapidly progressive disease course and SIVE
90 ranged from 25% to 90%. Studies in our laboratory have also shown that encephalitis
91 can be caused by using animals infected with the highly pathogenic virus isolate
92 SIVsmE660 or molecular clone, SIVsmE543.3 (24). Moreover, all of the animals which
93 were RP also exhibited SIVE (Brown and Hirsch in press). However, in recent work, we
94 observed SIVE in two rhesus macaques, inoculated with virus isolated from a
95 SIVsmE543-3–inoculated RP macaque, which survived greater than a year from
96 inoculation. This situation more likely parallels that of HIV-infected patients who do not
97 develop HIVE/dementia until late stage AIDS than do rapid progressor animals with
98 SIVE.

99 In the present study, we evaluated the sequential genetic and biologic evolution of
100 SIV in the plasma, cerebral spinal fluid (CSF), and brain from these conventional
101 progressors with encephalitis. Analyses of isolated viruses suggested diverging viral
102 evolution and different selective pressures in the plasma and CSF resulting in
103 compartmentalization of these viruses. Additionally, we observed a preferential
104 infection of primary rhesus monocyte-derived macrophages (MDM) versus peripheral
105 blood mononuclear cells (PBMC) by viruses isolated from CSF and brain. Conversely,
106 viruses isolated from plasma more efficiently infected PBMC than did viruses isolated
107 from CSF or brain. These viruses provide a relevant model to study the adaptations
108 required for SIV to induce encephalitis.

109

110

MATERIALS AND METHODS

Viruses and Macaques. SIVsmE543-3, a well-characterized pathogenic molecular clone was derived from a terminal PBMC sample of rhesus macaque E543 which had SIVE and AIDS (24). This virus was used to intravenously inoculate rhesus macaque H445. Macaque H445 rapidly progressed to disease with SIVE and was subsequently euthanized at 16 weeks postinoculation (21, 29). Virus stock was isolated from the mesenteric lymph node obtained at euthanasia by co-culture with naïve rhesus PBMCs and is designated SIVsmH445.

A cohort of six naïve rhesus macaques was then inoculated intravenously with 2000 $TCID_{50}$ of SIVsmH445. One of the animals, H635 developed typical rapidly progressive disease whereas the other five were normal progressors. Of these five, only H631 and H636 had histologic evidence of SIVE. All animals were housed in accordance with the NRC Guide for the Care and Use of Laboratory Animals (10).

***In situ* hybridization**: Formalin fixed, paraffin embedded tissues were stained for SIV RNA utilizing a method previously described (26). Briefly the sections were deparaffinized, pretreated with 0.2N HCL, proteinase K, and hybridized overnight at 50°C with either sense or anti-sense SIVmac239 digoxigenin-UTP labeled riboprobe (Lofstrand Labs). All probes were used at a final concentration of 1.75 ng/µl. The hybridized sections were washed in standard posthybridization buffers and RNase solutions, Ribonuclease A (Sigma) and RNase T1 (Roche Molecular). The sections were blocked with 3% normal sheep and horse serum in Tris, pH 7.4 and then incubated with sheep anti-digoxigenin-alkaline phosphatase, 1:500, (Roche Molecular) for 1hr. The sections were reacted with NBT/BCIP (Vector Laboratories, Ltd.) for 10hr. The samples

were rinsed with distilled water, counterstained with nuclear fast red (Sigma), and examined with a Zeiss Axiophot microscope equipped with a CoolSnap digital camera. Negative controls included mock hybridization, sense probe applied to infected tissues, anti-sense probe on uninfected tissues.

Immunohistochemistry. Tissue sections were stained for viral SIV RNA as outlined above with the following modifications. All samples were treated with a methonolic-hydrogen peroxide solution to quench endogenous peroxiadase prior to sheep anti-digoxigenin-horse radish peroxidase (Roche Molecular) followed by tyramide signal amplification (TSA). After the tyramide-FITC (Perkin Elmer) amplification, samples were incubated with anti-human CD3 (DAKO A0452), anti- human CD8 (Novocastra NCL-CD8-295), anti-human CD20 (Dako M0755), or anti-human HAM56 (DAKO M0632) for T-cell, B cell, or macrophage detection, respectively. Biotinylated secondary antibodies (Vector Labs) and streptavidin-Alexa 633 (Molecular Probes) were used to visualize the antibody stain. Samples were then counterstained with hematoxylin. Negative controls included mock hybridization, sense probe applied to infected tissues, anti-sense probe on uninfected tissues, omission of primary antibodies, omission of TSA-FITC and streptavidin-Alexa 633. All tissue sections were then mounted in Vectashield (Vector Labs) media viewed and photographed on a Lecia scanning laser confocal microscope (NIAID, NIH Core Facility).

Confocal Microscopy. Formalin-fixed, paraffin-embedded tissues were stained for SIV viral RNA by ISH as described above. Briefly the sections were deparaffinized, rehydrated, methanol-hydrogen peroxide, 0.2N HCl, proteinase K, and hybridized overnight at 50°C the anti-sense SIV_{mac239} digoxigenin-UTP labeled riboprobe. The

hybridized sections were blocked with 3% normal sheep and horse serum in 0.1M Tris, pH 7.4 and then incubated with sheep anti-digoxigenin-horseradish peroxidase (SAD-HRP, Roche Molecular Biochemicals). SAD-HRP was detected with a fluorescent tyramide signal amplification technique (TSA Plus FITC, PerkinElmer, NEL741). After completion of the ISH assay, the sections were incubated in mouse anti-human macrophage (HAM56, DAKO M0632) and stained with goat anti-mouse-IgM-Alexa633 (Invitrogen). The samples were then incubated with rabbit anti-human CD3 (T-cell marker, DAKO A0452) followed by goat anti-rabbit-IgG-Alexa594.

Western Blot Assay. Virus lysates were generated from infecting CEMx174 T cells with SIVsmE543-3. Equal amounts of SIVsmE543-3 lysate were mixed with 2X Laemmli Sample buffer. This preparation was boiled for four minutes and then cooled on ice before being loaded onto a 10% SDS-PAGE gel. The gel was run for 16 hours at 50-60V. The proteins were transferred for 48 hrs using a passive transfer technique onto a Hybond-P PVDF transfer membrane (Amersham Pharmacia). The transfer membrane was then washed, dried, and cut into strips. Two mililiters of diluent containing Tween, BSA, and PBS were added to each strip along with 20µl of sample serum from each monkey taken at sequential time points. The strips were incubated at room temperature for one to two hours, washed, and incubated for another hour with peroxidase conjugated immunopure protein A/G, (Pierce Biotech.). After another wash, the strips were developed using the BCIP/NBT Phosphatase Substrate System (Kirkegaard & Perry Labs).

Viral RNA Quantification. Viral RNA was isolated from either CSF or plasma samples using the QIAamp viral RNA mini kit (Qiagen, Hilden, Germany). Reverse

transcription was carried out using TAQMAN reverse transcription reagents (Applied Biosystems, Foster City, CA). Primers used for the RT-step were S-GAG03 and S-GAG04 and the probe was P-SUS-05. Viral RNA levels in the cerebral spinal fluid (CSF) and plasma were then determined by quantitative real-time PCR using the ABI Prism 7900HT sequence detector (Applied Biosystems, Foster City, CA). A more detailed protocol has previously been reported (27).

Virus Isolation and Replication Assay. To isolate virus, samples of cryopreserved CSF and plasma collected at week 76 (H636) and at euthanasia (week 116, H631) were incubated with primary pig-tail macaque PBMC. Additionally, for H631, virus was isolated from brain samples obtained during euthanasia. Cryopreserved brain was thawed and homogenized in Hank's balanced salt solution. This solution was spun down to pellet the cells and the resultant supernatant was filtered through a 0.45μm pore size filter before incubating with primary pig-tail macaque PBMC. PBMC culture supernatant was filtered to generate cell-free virus stocks and RT assay (see below) was performed to normalize all virus stock.

For virus replication assay, Ficoll-Hypaque density gradient centrifugation of EDTA-treated whole blood from four different rhesus macaques, H705, HM03, HCL16, and HCL27, was performed to isolate PBMC. Four donors were used to prevent donor bias. Cells were stimulated with 2 μg of PHA (Sigma) per ml and 5 half-maximal units per ml of human interleukin-2 (Advanced Biotechnologies, Columbia, Md. in RPMI 1640, supplemented with 10% heat-inactivated FCS, 2 mM glutamine, 100 U of penicillin per ml, 100 μg of streptomycin per ml, and 10 mM HEPES for 3 days and then washed and maintained in complete RPMI 1640 supplemented with 10% IL-2 for one day before

infection. Additionally, MDM were cultivated from 1.5 x 10^6 PBMC in RPMI 1640 medium containing inactivated fetal calf serum (15%), human type AB serum (10%) (Sigma) and human M-CSF (500U/ml) (R&D Systems, Inc.) for five days. The wells were then washed to remove non-adherent cells and maintained in medium containing inactivated fetal calf serum (15%), human type AB serum (5%), and human M-CSF (200U/ml) for two more days. Just prior to infection, both PBMC and MDM were washed. For infection studies, 2.5×10^5 PHA-stimulated PBMC were infected in 48-well plates. Virus amounts corresponding to100,000 counts per minute (cpm) of RT activity were used to infect both PBMC and MDM for three hours at which time, the cells were washed to remove non-attached viruses. Every three days for three weeks, one half of the culture supernatant was removed for analysis and replaced with fresh medium.

Reverse Transcriptase Assay. An aliquot of cell-free virus-containing supernatant was removed every three days from infected cells and frozen at -80°C. After all experiments were completed, the cell-free virus-containing supernatants were used to measure virion-associated reverse transcriptase (RT) activity. The RT assays were all performed at the same time in order to ensure that the results could be compared with each other. For each virus, 15µl of culture supernatant was added to a reaction mix (50µl) containing: 50mM Tris (pH 7.8), 75mM KCl, 2mM dithiothreitol, 5mM MgCl2, 5µg/ml Poly A (Amersham Pharmacia), 6.2µg/ml Oligo dT (GE Amersham), 0.05% Nonidet P-40 (Sigma), 0.5mM EGTA, and 20µCi/ml P^{32} dTTP, (800 Ci/mmol, GE Amersham). The reaction mix was incubated in a humidified chamber at 37°C for 1.5 hr, upon which time, 10µl was dotted onto Whatman DE81 anion exchanger paper. After drying, the Whatman paper was washed five times in a solution containing 0.15 M NaCl

and 0.015 M sodium citrate to remove any unincorporated P^{32} dTTP. The Whatman paper was rinsed a final time with 100% ethanol, dried, and the amount of radioactivity incorporated was quantified using PhosphoImager (Fuji).

Sequence and Phylogenetic Analyses. Viral RNA was isolated from sequential CSF and plasma samples, as well as from isolated viruses, using QIAamp viral RNA mini kit (Qiagen, Hilden, Germany) according to manufacturer's instructions. All viral RNA was treated with DNase I prior to RT-PCR, which was performed using the one step RT-PCR for long templates kit (Invitrogen, Carlsbad, CA). Primers 9734 (5'-GCA ATG AGA TGT AAT AAA ACT G-3') and 9737R (5'-GGT GCC TCA AGA AAT AAG AGA G-3') were used to amplify the gp120 region of envelope. Additionally, primers 6463 (5' GGT GTT GCT ATC ATT GTC AGC-3') and 9341R (5'-CAT CAT CCA CAT CAT CCA TG) were used to amplify the entire envelope region and the PCR product was inserted into a cloning vector using the TOPO TA kit (Invitrogen). To avoid amplification error bias of the template, the PCR reaction was performed three to four times and several clones were chosen for sequencing from each PCR reaction for an average total of nine to ten clones per tissue sample per time point. The only exception to this was for CSF from animal H636 at week 32 p.i., where only four clones were sequenced. Additionally, eluted PCR products were visualized using crystal violet, not ethidium bromide to prevent any possible mutations caused by intercalation of ethidium bromide into the DNA. Sequencing of the gp120 region from sequential tissue samples was performed using the following primers: M13F, M13R (M13F and M13R are Topo TA cloning primers), SM19 (5'-AAC AAC AGT AAC ACC AAA GG-3'), SM20 (5'-TAC TTG GTT TGG CTT CAA TGG-3'), and SM21 (5'-GGT TTC TCA ATT GGG

249 TAG AG-3'). Sequencing of the entire envelope from the isolated viruses was performed
250 using the following primers:6463, 9734, SM20, SM21, SM22 (5' TTC TCG CGA CAG
251 CAG GTT CTG-3'), SM23 (5'-GAA TTG CAA AAA CTA AAT AGC-3'), SM24 (5'-
252 GTG CTC CAG AGA CTC TCA AG-3'), and 9341R. Sequencing was performed on the
253 Applied Biosystems 3130XL Genetic Analyzer.

254 Alignment of sequences was done using MUSCLE (13) and manually edited with
255 BioEdit v5.0.9 (23). Columns containing gaps in the alignment were stripped prior to
256 phylogenetic analyses. A maximum likelihood tree incorporating site-specific nucleotide
257 substitution rates from an alignment of nucleotide sequences was constructed using
258 PHYLIP (17) and DNArates 1.1.0 (Olsen, G. J., Pracht, S., and Overbeek, R.,
259 unpublished). In addition, a transition/transversion ratio of 1.5 was used in the analyses.
260 The tree was rooted on the parental SIVsmE543-3 sequence (accession no. U72748).
261 Maximum likelihood bootstrapping support values were calculated using 1000 replicates
262 with PHYLIP.

263 Synonymous/non-synonymous analysis program (SNAP) (37),
264 http://www.hiv.lanl.gov/content/hiv-db/SNAP/WEBSNAP/SNAP.html was used to
265 calculate the synonymous and non-synonymous substitution rates based on a set of
266 codon-aligned nucleotide sequences. This program was based on the method of Nei and
267 Gojobori (50) and incorporated a statistical analysis developed by Ota and Nei (54).

268 Potential N-linked glycosylation sites (PNGS) were analyzed by the LANL N-
269 Glycosite program (http://www.hiv.lanl.gov/content/hiv-
270 db/GLYCOSITE/glycosite.html). Comparison of the number of PNGS in Env of H631
271 virus isolates and H636 CSF virus isolates to SIVsmE543-3 Env was performed using

one sample T test, two tailed. Comparison of the number of PNGS in Env of H631 brain virus isolates to that of H631 CSF or plasma virus isolates was performed with unpaired two sample T test, two tailed. P values < 0.05 were reported as significant.

RESULTS

As part of prior ongoing studies, rhesus macaque H445 was inoculated intravenously with the pathogenic molecular clone, SIVsmE543-3 (24). Following inoculation, H445 developed a transient antibody and cytotoxic T lymphocyte (CTL) response and had high plasma and tissue viral load. This animal rapidly progressed to AIDS with euthanasia occurring at week 16 post inoculation (p.i.) (21). Previous studies have suggested that virus passaged in macaques have evolved to become more virulent (6, 15, 25, 31, 33, 68) Therefore, we sought to evaluate the pathogenicity of SIV isolates from tissues of this rapid progressor. Uncloned virus was then isolated from the mesenteric lymph node of H445 at euthanasia by co-culture with naïve rhesus PBMC and inoculated intravenously into a cohort of six rhesus macaques (39).

All six animals became infected and had clinical and pathological symptoms characteristic of SIV-related disease (39). Although six animals were inoculated with virus isolated from a RP, only H635 progressed rapidly with characteristic immunopathology (29) and was subsequently euthanized at week 9 p.i. (39). The survival time of the other five conventional progressor animals ranged from 52 to 116 weeks p.i. (39).

As shown in Figure 1A, high levels of plasma viral RNA were detected in all animals during primary viremia, ranging from 10^7 to 10^9 copies per ml. These levels

295 generally decreased by one to two logs by week 4 p.i. and were maintained at these
296 levels until death (Fig. 1A). The rapid progressor macaque, H635 was the one exception,
297 showing increasing viral load until death. Detection of viral RNA in the CSF was
298 observed by week 1 p.i. and measured at 10^5 to 10^6 copies per ml during primary
299 infection in all macaques. For H632, H633, and H634, viral RNA in sequential CSF
300 samples remained at moderate to low levels. However, for H631, H635, and H636, CSF
301 viral RNA levels increased terminally to 10^7 to 10^8 copies per ml (Fig. 1B).
302 To monitor the immune status of the animals, the number of $CD4^+$ T cells per μl
303 of blood was measured by flow cytometry. In all cases, the level of $CD4^+$ T cells fell
304 sharply during primary infection but then rebounded. Only in H635, did $CD4^+$ T cell
305 levels recover back to normal by death. However, in the other five animals, $CD4^+$ T cell
306 levels gradually declined terminally after the initial recovery, with a mean level of 198
307 cells/μL at the time of euthanasia (data not shown).
308 With the exception of H635, all macaques developed moderate to robust
309 responses to SIV-Gag by week eight and to SIV-Env (gp160) by week 32 (data not
310 shown). We did not detect SIV-specific antibodies for H635 (data not shown). This is
311 consistent with characteristics of RP which can have transient to undetectable immune
312 responses (12, 29).
313 **Encephalitis Observed in Two Conventional Progressors.** Histological
314 examination of brain obtained during either necropsy or autopsy of all six animals
315 revealed that half of the cohort developed SIV meningoencephalitis (39). SIVE in these
316 three animals was characterized by perivascular cuffing and MNGC, the latter considered
317 the hallmark of encephalitis. Perivascular lymphocytic cuffing was observed in the

318 brains of the two conventional progressors, H631 and H636, a pathologic feature not
319 observed in the rapid progressor brain sections. Immunohistochemistry using anti-CD20
320 and anti-CD3 antibodies, demonstrated that the infiltrating cells consisted of B and T
321 cells, respectively, and that these latter cells were predominantly $CD8^+$ T cells (Fig. 2).
322 In contrast, only occasional T cells and no B cells were observed in the brain of the rapid
323 progressor macaque, H635. As also shown in Fig. 2, infiltrating macrophages and
324 MNGC were identified by HAM56, a macrophage marker, and these cells co-localized in
325 lesions with SIV expression, as shown by in situ hybridization (ISH). Triple label
326 confocal microscopy using ISH for SIV RNA and immunofluorescence for HAM56 and
327 anti-CD3 demonstrated that the SIV-expressing cells in the brain were macrophages.
328 **Molecular evolution of SIV.** To determine whether specific SIV variants were
329 associated with the development of SIVE in these three animals, we examined the Env
330 sequence of viral RNA amplified directly from CSF and plasma of H631, H636 and
331 H635 and compared it to the inoculum, SIVsmH445. The SIVsmH445 virus inoculum
332 stock showed few changes in the gp120 region of Env as compared to the parental
333 SIVsmE543-3 (39). Of the few mutations observed, the majority were characteristic
334 rapid progressor-specific mutations (12, 39) that we have described previously in rapid
335 progressor macaques. However, clones with these mutations were a minority
336 population. Analyses of sequences obtained directly from CSF (data not shown) and
337 plasma (39) of the rapid progressor macaque, H635 at the time of death showed that that
338 RP-specific mutations predominated in both compartments, consistent with specific
339 selection of this minority viral variant from the inoculum. In contrast, sequencing of CSF
340 and plasma from H631 and H636 did not reveal RP-specific mutations in any of the

341 clones analyzed at any time point. Consequently, we have used the parental SIVsmE543-
342 3 sequence for comparisons.

343 Viral RNA was isolated directly from CSF and plasma of H631 and H636 at
344 sequential time points during primary viremia and up to and including death (H631).
345 Animal H636 died unexpectedly; consequently, only samples from the last time point at
346 week 76 p.i. were available. Sequencing analysis of the gp120 region of the viral
347 envelope amplified by RT-PCR revealed that virus during primary viremia in both
348 compartments for both animals had few and random mutations compared to that of
349 SIVsmE543-3. However, by week 32 p.i., mutations primarily in the V1 and V2 regions
350 of gp120 could be observed (Fig 3) with extensive changes seen by week 76 p.i.. These
351 mutations consisted of substitutions and insertion/deletion polymorphisms. Mutations
352 were also observed in the V4 region (data not shown).

353 By week 32 p.i. in H631 CSF and plasma clones (Fig 3A), except for two
354 substitutions (S193A and N215D) in CSF, there were no consistent mutations observed in
355 the V1 and V2 regions of gp120. Interestingly, the CSF S193A and N215D substitutions
356 were maintained through death (week 116 p.i.). The latter mutation resulted in a loss of a
357 potential N-linked glycosylation site (PNGS). This suggests that these mutations may
358 have conferred a selective advantage for viral fitness to the virus in H631 CSF. By week
359 76 p.i., many more mutations were observed for both CSF and plasma clones. The
360 majority of the mutations were different for the two compartments, with CSF clones
361 having changes in both V1 and V2 regions and plasma clones having changes
362 concentrated more heavily in the V1 region. However, two substitutions were found to
363 be consistent in both H631 CSF and plasma. These were the A133T in V1, and the

364 P201S outside of the V2 region. Many changes that were observed at week 76 were also
365 observed at death; however, there were still new and different mutations at death as
366 compared to week 76 suggesting that the virus in H631 CSF and plasma continued to
367 evolve. One such change is the seven amino acid insertion seen in three of the CSF
368 clones. This insertion was due to a duplication of the downstream animo acids and
369 resulted in a new PNGS.

370 In contrast, there appeared to be fewer mutations overall in H636 clones (Fig 3B)
371 than in H631, and there were no consistent changes that were maintained from week 32
372 p.i. to week 76 as seen in H631. Mutations observed in CSF and plasma at week 32 p.i.
373 were replaced by different mutations by week 76 p.i. Interestingly, in several instances,
374 the same mutations were found in both CSF and plasma compartments. At week 32 p.i.,
375 a K134N substitution resulted in a new PNGS, but was subsequently lost at the next
376 timepoint. At week 76 p.i., two substitutions were observed in both the V1 and V2
377 regions. These were the T139I and the K184E changes, respectively. Additionally, a
378 S206N substitution caused a shift in the PNGS originally at position 204. Overall, these
379 data suggest that virus in H636 was possibly under different selective pressures at these
380 two time points.

381 Phylogenetic analyses were then performed to study the relationship of these
382 sequences. Alignment of sequences as compared to SIVsmE543-3 was used to generate
383 trees that were constructed using DNA maximum-likelihood method. Incorporation of
384 site-specific nucleotide substitution rates were also used in the analyses (Figure 4).
385 Consistent with the observed sequence alignment shown in Fig. 3, phylogenetic analysis
386 of gp120 sequences at the terminal timepoint, demonstrated that SIV evolved differently

387 in the two macaques with sequences from H631 forming a distinct cluster, separate from
388 that of H636 (data not shown). Based on these results, all subsequent analyses were then
389 performed to show the different evolution occurring in each animal.

390 Sequences obtained from H631 CSF, shown in blue symbols and plasma viral
391 RNA, shown in red symbols (Fig. 4A) were found to be clustered based on their time
392 points at week 1 and 32. At week one, CSF and plasma sequences (triangles) were still
393 closely related to one another and to SIVsmE543-3, indicating that very little evolution
394 occurred. At week 32 (circles), CSF and plasma sequences for the most part, formed
395 their own clade suggesting that selective pressures in these compartments may have been
396 different from that of week 1. Viral sequences isolated at week 76 (squares) and at death
397 (stars) continued to diverge from week 32, but were quite related to one another, thus
398 implying that immune pressure from week 76 to week 116 was still a factor in their
399 evolution. It is important to note however, that virus from CSF and virus from plasma
400 remained clustered based on their respective compartment.

401 Similar to what was observed at week 1 in H631, CSF and plasma sequences in
402 macaque H636 were also very similar to one another and to SIVsmE543-3 (Fig. 4B). By
403 week 32, while virus could be seen to have diverged from SIVsmE543-3, CSF and
404 plasma sequences did not form their own clades. Half of the sequences from plasma at
405 week 76 appear to be direct descendents of virus from plasma at week 32. In contrast,
406 the other half, possibly under different selective pressures, had formed a different clade
407 with virus from CSF.

408 To determine if the changes observed in the gp120 sequences were due to random
409 mutations or due to positive selection from immune pressure, the rate of nonsynonymous

410 (dN) to synonymous (dS) change was calculated for each clone at sequential timepoints
411 and the average ratio is shown in Table 1. Positive selection is evidenced by a dN/dS
412 ratio > 1. In macaque H631, increasing positive selection could be seen in both CSF and
413 plasma gp120 sequences throughout the course of infection, with positive selection
414 occurring by week 76. Strong positive selection was evident by death indicating that
415 immune pressures in these compartments drove the evolution of these viruses in H631.
416 In the case of macaque H636, increasing positive selection was also observed for plasma
417 sequences; however, with sequences obtained from CSF, only slight positive selection
418 was seen by week 32, but had weakened slightly by week 76.

419 **Replicative abilities of viruses isolated from H631 and H636.** To study the
420 biological consequences of the observed mutations, we isolated virus from CSF and
421 plasma from both animals at the terminal time point. In the case of H636, since this
422 animal died unexpectedly, only samples from CSF and plasma obtained at week 76, three
423 weeks prior to death, were available. For H631, due to a decline in the animal's health, a
424 planned necropsy was performed at week 116. This allowed us to obtain samples from
425 not only the CSF and plasma, but from the brain as well. Virus was then isolated by
426 incubation of the respective tissue with fresh primary macaque PBMC.

427 To evaluate the replicative ability of the isolated viruses, PBMC from a donor
428 rhesus macaque were used in an infectivity assay and infection was monitored by RT
429 activity of culture supernatants followed by quantification using phosphorimaging
430 techniques. A representative infection is shown in Figure 5A-B. Virus isolates from
431 H631 brain, CSF, and plasma (Fig. 5A), as well as from H636 CSF and plasma (Fig. 5B)
432 were all able to infect PBMC. However, the replication efficiency varied among the

viruses. Virus from both H631 plasma and H636 plasma (shown in black) were found to replicate much more efficiently than the corresponding virus from the central nervous system (CNS) (shown in red) of the same animal. E543-3 was used as a control (shown in gray).

Based on our earlier observation of SIV-infected macrophages in the brain, we then wanted to evaluate viral replication in MDM. All experiments were performed in the same manner and a representative infection from one macaque donor is shown in Fig. 5C-D. Again, all viruses from both animals were able to replicate in MDM. However, in contrast to what was observed in the PBMC infections, infectivity of MDM by virus isolated from CNS of both macaques was much higher than that of virus isolated from PBMC.

To ensure that there were no donor biases as different macaques may have variable susceptibilities to infection (21), this infectivity assay was repeated using an additional three different donor macaques. The same donor macaques were used in both the PBMC and MDM experiments. Data from the four different infection assays were then combined to obtain an average, and the experiment was then independently repeated a second time. The results shown in Fig. 6 were determined from the average of these two independent experiments and thus gave a better assessment of their replicative ability. These experiments confirmed the initial results and demonstrated a marked trend for virus isolated from plasma of either H631 (Fig.6A) or H636 (Fig. 6B) to replicate in PBMC better than their counterpart virus isolated from the CNS. Similarly, replication of viruses isolated from CNS was observed to infect MDM better than virus isolated from

455 plasma (Fig. 6C and 6D). Thus, our data suggests that there is a preference for cell
456 tropism that is dependant on the origin of the virus compartment.

457 **Phylogenetic analyses of isolated viruses.** Based on the observed differences in
458 biological phenotypes, we wanted to examine the viral sequences to evaluate the
459 phylogenetic relationships of the isolated viruses. Viral RNA was isolated and RT-PCR
460 was performed to amplify the entire envelope region (gp160). Similar analyses as
461 described above were performed. Additionally, bootstrapping support tests based on
462 DNA maximum likelihood method were done to examine the reliability of the topology
463 or branching order of the tree. Bootstrap support values were based on 1000 replicates
464 and only values greater than 70% at the major nodes are shown. The phylogenetic tree
465 shown in Fig. 7A depicts the relationship of gp160 sequences derived from the viruses
466 isolated from H631 brain (green symbols), CSF (blue), and plasma (red) as compared to
467 SIVsmE543-3. With the exception of one envelope clone obtained from a plasma virus,
468 all sequences from each of the three compartments clustered within their respective
469 groups. However, despite the fact that the viruses were quite distinct and formed their
470 own clades, bootstrap values did not support that viruses from brain, CSF, and plasma
471 were compartmentalized. For macaque H636, phylogenetic analyses and bootstrap
472 support tests indicated that viruses from the CSF and plasma compartments were indeed
473 compartmentalized (bootstrap values 916 and 736, respectively) (Fig. 7B).

474 In contrast to H631 and H636, gp160 sequences amplified directly from CSF and
475 plasma viral RNA of H635, a rapid progressor with SIVE, indicated that there was
476 intermingling of virus between plasma and CSF and no tissue-specific localization of
477 virus (Fig. 7C).

478 The rates of nonsynonymous to synonymous changes were also calculated for
479 H631 and H636 isolated viruses. For all cases, the dN/dS ratio was greater than one,
480 indicating that positive selection was responsible for the evolution of these viruses (data
481 not shown).

482 **Loss of potential N-linked glycosylation sites.** Sequencing analyses revealed
483 that there were changes in the potential N-linked glycosylation site (PNGS) pattern as
484 compared to SIVsmE543-3 (Fig 3 and data not shown). To investigate the number of
485 PNGS in Env of the virus isolates, we used the N-glycosite program (73) to determine
486 that there was a statistically significant loss of PNGS in gp160 of all H631 virus isolates
487 and H636 CSF virus isolates compared to SIVsmE543-3 (one sample T test, two tailed, *P*
488 values ranged from $P< 0.0001$ to $P<0.0054$) (Fig. 8). Furthermore, the number of PNGS
489 in Env of H631 brain virus isolates was found to be lower than that of H631 CSF and
490 plasma virus (unpaired two sample T test, two tailed, $P< 0.0001$ and $P<0.0005$,
491 respectively).
492
493 **DISCUSSION**
494 In terms of SIV neuropathogenesis studies, there are primarily three macaque
495 models that have been shown to reliably induce neuroAIDS (52, 61, 74). These studies
496 have appeared to focus mainly on macaques with rapid progressive disease and
497 encephalitis. In contrast, in the current study, we present data on two animals with
498 conventional progressive disease having SIVE. While this phenomenon occurs much less
499 frequently than that of rapid progressors with SIVE, it has been observed by others using

500 different virus inocula (5, 51, 52, 62). However, this is the first report with animals
501 infected with a derivative of SIVsmE543-3.

502 To better understand the virologic factors that may contribute to this finding, we
503 analyzed viral RNA representing the gp120 region of envelope from CSF and plasma of
504 H631 and H636 at sequential time points. This allowed us to study the evolution of
505 actively replicating viruses These analyses demonstrated that during the acute phase of
506 infection (week 1 p.i.) viruses from CSF and plasma in their respective hosts, were
507 phylogenetically very similar to one another. This indicated a systemic spread by the
508 inoculum, with seeding from the periphery to the CNS since the animals were inoculated
509 by intravenous route. However, as disease progressed in H631, divergent evolution in the
510 two compartments was observed by week 32 p.i. and continued until death. For H636,
511 divergent evolution between CSF and plasma was more evident by terminal disease.
512 With the exception of H636 CSF, increasingly positive selection was observed for the
513 changes seen in the genotypes, suggesting that immune selection pressures or lack
514 thereof, continued to drive the evolution of SIV in these macaques.

515 Additionally, we analyzed viral RNA representing the entire envelope from
516 viruses isolated from different compartments at endstage disease. Phylogenetic analyses
517 of the isolated viruses showed that there was divergent evolution among the different
518 compartments confirming what was seen in analyses examining direct tissue. Moreover,
519 bootstrap support values indicated compartmentalization of H636 viruses. Despite H631
520 viruses clustering together (with the exception of one clone from plasma) in their own
521 clade, bootstrap values did not indicate compartmentalization. This is not altogether
522 surprising as we expected brain and CSF viral sequences to be more closely related to

523 one another and therefore were not supported by bootstrap analyses. However, when the
524 phylogenetic relationship was re-analyzed but excluded sequences from brain, similar to
525 what was observed with H636 viruses, bootstrap values did support compartmentalization
526 between viruses isolated from CSF and plasma (722 and 943, respectively, data not
527 shown).

528 The observation of independent localized evolution of envelope in different
529 tissues from the same monkey or individual has been previously reported for SIV (5, 62)
530 and HIV-1 (38, 53). Interestingly, analysis of viral RNA isolated from direct tissues
531 obtained during autopsy of H635, a rapid progressor macaque with SIVE, showed that
532 the envelope sequences between CSF and plasma viruses were very similar to one
533 another with no monophyletic clades being formed. One would not expect to see
534 compartmentalization as disease progression is so rapid. The lack of
535 compartmentalization is also consistent with major dysfunction of the blood-brain barrier
536 in rapid progressor macaques with SIVE where the distribution of SIV can be found
537 throughout the brain parenchyma (unpublished data) (52). In contrast, SIV was primarily
538 localized to the perivascular regions in macaques H631 and H636. Furthermore, the
539 pathology of the brain of these two conventional progressors was significantly different
540 from that of H635 (which did not have lymphocytic infiltrates), with the presence of
541 prominent perivascular mononuclear infiltrates containing both T and B cells. The
542 presence of lymphocytes is more similar to the pathology of HIVE (2, 32, 45, 56, 57).
543 These differences support a SIV/macaque model for neuroAIDS using conventional
544 progressors with SIVE rather than rapid progressors with SIVE.

545 The biological consequences of the tissue-specific genotypes were evaluated in
546 infectivity assays using primary, naïve macaque PBMC and MDM. We observed that in
547 matched pairs of virus isolates that virus from CNS was able to more efficiently infect
548 MDM in comparison to PBMC. Conversely, virus isolated from plasma was able to
549 replicate better in PBMC than in MDM. Our results agree with a previous report where
550 paired CNS and PBMC HIV-1 virus isolates from the same individual were also found to
551 have a preference in cellular tropism based on their origin (7).
552 From our phylogenetic analyses, our data strongly suggest that the inoculum
553 evolved over time in different compartments under different local selective pressures
554 resulting in divergent evolution of virus. Consequently, virus from brain/CSF adapted to
555 preferentially infect MDM and virus from plasma was better suited to infect PBMC.
556 Perivascular macrophages have been shown to be the primary cell type productively
557 infected by HIV-1 and SIV in the brains of humans and macaques with lentivirus-induced
558 encephalitis (18, 72). Thus our observations extend and support the notion that viruses
559 isolated from CNS would evolve to selectively infect macrophages.
560 Given that expression of CD4 levels on human and macaque macrophages are low
561 to undetectable (46, 71, 72), it is possible that this adaptation may be due to the selection
562 of viral strains that have less dependence on using CD4 for entry. Indeed, both SIV and
563 HIV viral variants have been reported previously to be CD4-independent by infectivity
564 assays (14, 36). Moreover, CD4 independence has been associated with a loss of
565 potential N-linked glycosylation sites (PNGS) (35, 47). The finding that there was a
566 statistically significant loss of PNGS in gp160 in H631 and H636 CSF virus isolates, and
567 in particular, in H631 brain virus isolates, may be explained by the fact that the brain is a

568 selectively immune-privileged site. Therefore, it is reasonable to assume that H631 virus
569 in this compartment may adapt to decrease the number of PNGS given that they are less
570 likely to encounter humoral immune pressure.

571 A study analyzing 37 full length HIV-1 Env clones sequenced from uncultured
572 brain and blood from four patients with late stage AIDS reported tissue-specific
573 compartmentalization of virus; however, no significant difference in the number or
574 position of PNGS was observed between blood and brain Env sequences (53). This is in
575 contrast to our data. While the HIV study used samples from patients in late stage AIDS,
576 these patients did not have HIVE. Moreover, viral DNA were utilized for the
577 phylogenetic analyses and consequently, the sequences used may not accurately represent
578 the actively replicating viral variants. Samples used in our study were from macaques
579 with SIVE and we isolated viral RNA to examine the viral strains replicating at the time
580 of isolation. Thus this may explain the difference in results. Additionally, we can not
581 rule out the possibility that other mutations may have allowed for increased fitness for
582 replication in the brain. More analyses are needed to determine the mutation(s) important
583 for this finding.

584 We (24) and others (19, 20, 62) have previously reported the observation of a
585 premature stop codon resulting in the truncation of the transmembrane gp41 envelope
586 protein in the brains of macaques with SIVE. Recently, this truncation in addition to a
587 single amino acid substitution (arginine to glycine, also in the gp41 region) was found to
588 be sufficient for CD4-independent entry for SIV (4). However, in the current study, we
589 did not observe any truncation of gp41 protein in both the brain and CSF envelope
590 (gp160) sequences for both H631 and H636. In all of the above studies, DNA was used

591 to amplify the envelope region whereas we isolated RNA and performed RT-PCR to
592 amplify this region. Thus using genomic DNA may reflect viral variants which might be
593 latent as well as actively replicating.

594 In summary, we have isolated viruses from the brain and CSF of two conventional
595 progressor macaques with neuroAIDS. Our data demonstrated the importance of the
596 environment on the selection of particular genotypes from quasispecies. Indeed, these
597 viruses appear to have undergone adaptive evolution to efficiently replicate in the CNS.
598 Future studies are planned to study whether the viruses can be neuroviruluent in
599 macaques and to examine the molecular determinants which may contribute to
600 neurological disease.

601

602 **ACKNOWLEDGEMENTS**

603 We thank Sonya Whitted and Christopher Erb (LMM, NIAID) for technical
604 assistance. This work was supported by the intramural program of the National Institute
605 of Allergy and Infectious Diseases.

606 **REFERENCES**

607 1. 1991. Nomenclature and research case definitions for neurologic manifestations
608 of human immunodeficiency virus-type 1 (HIV-1) infection. Report of a Working
609 Group of the American Academy of Neurology AIDS Task Force. Neurology
610 **41:**778-85.

611 2. **Anthony, I. C., D. H. Crawford, and J. E. Bell.** 2004. Effects of human
612 immunodeficiency virus encephalitis and drug abuse on the B lymphocyte
613 population of the brain. J Neurovirol **10:**181-8.

614 3. **Baskin, G. B., M. Murphey-Corb, E. D. Roberts, P. J. Didier, and L. N.**
615 **Martin.** 1992. Correlates of SIV encephalitis in rhesus monkeys. J Med Primatol
616 **21:**59-63.

617 4. **Bonavia, A., B. T. Bullock, K. M. Gisselman, B. J. Margulies, and J. E.**
618 **Clements.** 2005. A single amino acid change and truncated TM are sufficient for
619 simian immunodeficiency virus to enter cells using CCR5 in a CD4-independent
620 pathway. Virology **341:**12-23.

621 5. **Chen, M. F., S. Westmoreland, E. V. Ryzhova, J. Martin-Garcia, S. S.**
622 **Soldan, A. Lackner, and F. Gonzalez-Scarano.** 2006. Simian
623 immunodeficiency virus envelope compartmentalizes in brain regions
624 independent of neuropathology. J Neurovirol **12:**73-89.

625 6. **Chen, Z., Y. Huang, X. Zhao, E. Skulsky, D. Lin, J. Ip, A. Gettie, and D. D.**
626 **Ho.** 2000. Enhanced infectivity of an R5-tropic simian/human immunodeficiency
627 virus carrying human immunodeficiency virus type 1 subtype C envelope after
628 serial passages in pig-tailed macaques (Macaca nemestrina). J Virol **74:**6501-10.

7. **Cheng-Mayer, C., C. Weiss, D. Seto, and J. A. Levy.** 1989. Isolates of human immunodeficiency virus type 1 from the brain may constitute a special group of the AIDS virus. Proc Natl Acad Sci U S A **86:**8575-9.

8. **Cherner, M., E. Masliah, R. J. Ellis, T. D. Marcotte, D. J. Moore, I. Grant, and R. K. Heaton.** 2002. Neurocognitive dysfunction predicts postmortem findings of HIV encephalitis. Neurology **59:**1563-7.

9. **Clements, J. E., and M. C. Zink.** 1996. Molecular biology and pathogenesis of animal lentivirus infections. Clin Microbiol Rev **9:**100-17.

10. **Council, N. R.** 1996. Guide for the care and use of laboratory animals, [7th ed. National Academy Press, Washington, D.C.

11. **Daniel, M. D., N. L. Letvin, P. K. Sehgal, G. Hunsmann, D. K. Schmidt, N. W. King, and R. C. Desrosiers.** 1987. Long-term persistent infection of macaque monkeys with the simian immunodeficiency virus. J Gen Virol **68 (Pt 12):**3183-9.

12. **Dehghani, H., B. A. Puffer, R. W. Doms, and V. M. Hirsch.** 2003. Unique pattern of convergent envelope evolution in simian immunodeficiency virus-infected rapid progressor macaques: association with CD4-independent usage of CCR5. J Virol **77:**6405-18.

13. **Edgar, R. C.** 2004. MUSCLE: multiple sequence alignment with high accuracy and high throughput. Nucleic Acids Res **32:**1792-7.

14. **Edinger, A. L., J. L. Mankowski, B. J. Doranz, B. J. Margulies, B. Lee, J. Rucker, M. Sharron, T. L. Hoffman, J. F. Berson, M. C. Zink, V. M. Hirsch, J. E. Clements, and R. W. Doms.** 1997. CD4-independent, CCR5-dependent

infection of brain capillary endothelial cells by a neurovirulent simian immunodeficiency virus strain. Proc Natl Acad Sci U S A **94:**14742-7.

15. **Edmonson, P., M. Murphey-Corb, L. N. Martin, C. Delahunty, J. Heeney, H. Kornfeld, P. R. Donahue, G. H. Learn, L. Hood, and J. I. Mullins.** 1998. Evolution of a Simian Immunodeficiency Virus Pathogen. J. Virol. **72:**405-414.

16. **Epstein, L. G., L. R. Sharer, E. S. Cho, M. Myenhofer, B. Navia, and R. W. Price.** 1984. HTLV-III/LAV-like retrovirus particles in the brains of patients with AIDS encephalopathy. AIDS Res **1:**447-54.

17. **Felsenstein, J.** 2005. PHYLIP (Phylogeny Inference Package), 3.6 ed. Distributed by author. Department of Genome Sciences, University of Washington, Seattle, WA.

18. **Fischer-Smith, T., S. Croul, A. E. Sverstiuk, C. Capini, D. L'Heureux, E. G. Regulier, M. W. Richardson, S. Amini, S. Morgello, K. Khalili, and J. Rappaport.** 2001. CNS invasion by CD14+/CD16+ peripheral blood-derived monocytes in HIV dementia: perivascular accumulation and reservoir of HIV infection. J Neurovirol **7:**528-41.

19. **Flaherty, M. T., D. A. Hauer, J. L. Mankowski, M. C. Zink, and J. E. Clements.** 1997. Molecular and biological characterization of a neurovirulent molecular clone of simian immunodeficiency virus. J Virol **71:**5790-8.

20. **Glenn, A. A., and F. J. Novembre.** 2004. A single amino acid change in gp41 is linked to the macrophage-only replication phenotype of a molecular clone of simian immunodeficiency virus derived from the brain of a macaque with neuropathogenic infection. Virology **325:**297-307.

21. **Goldstein, S., C. R. Brown, H. Dehghani, J. D. Lifson, and V. M. Hirsch.** 2000. Intrinsic susceptibility of rhesus macaque peripheral CD4(+) T cells to simian immunodeficiency virus in vitro is predictive of in vivo viral replication. J Virol **74:**9388-95.

22. **Hahn, B. H., G. M. Shaw, K. M. De Cock, and P. M. Sharp.** 2000. AIDS as a zoonosis: scientific and public health implications. Science **287:**607-14.

23. **Hall, T.** 1997-2005. BioEdit 5.0.9 ed. Ibis Therapeutics, Carlsbad, CA.

24. **Hirsch, V., D. Adger-Johnson, B. Campbell, S. Goldstein, C. Brown, W. R. Elkins, and D. C. Montefiori.** 1997. A molecularly cloned, pathogenic, neutralization-resistant simian immunodeficiency virus, SIVsmE543-3. J Virol **71:**1608-20.

25. **Hirsch, V. M.** 1999. Evolution of the fittest ends in tragedy. Nat Med **5:**488-9.

26. **Hirsch, V. M., G. Dapolito, P. R. Johnson, W. R. Elkins, W. T. London, R. J. Montali, S. Goldstein, and C. Brown.** 1995. Induction of AIDS by simian immunodeficiency virus from an African green monkey: species-specific variation in pathogenicity correlates with the extent of in vivo replication. J Virol **69:**955-67.

27. **Hirsch, V. M., T. R. Fuerst, G. Sutter, M. W. Carroll, L. C. Yang, S. Goldstein, M. Piatak, Jr., W. R. Elkins, W. G. Alvord, D. C. Montefiori, B. Moss, and J. D. Lifson.** 1996. Patterns of viral replication correlate with outcome in simian immunodeficiency virus (SIV)-infected macaques: effect of prior immunization with a trivalent SIV vaccine in modified vaccinia virus Ankara. J Virol **70:**3741-52.

28. **Hirsch, V. M., and P. R. Johnson.** 1994. Pathogenic diversity of simian immunodeficiency viruses. Virus Res **32:**183-203.

29. **Hirsch, V. M., S. Santra, S. Goldstein, R. Plishka, A. Buckler-White, A. Seth, I. Ourmanov, C. R. Brown, R. Engle, D. Montefiori, J. Glowczwskie, K. Kunstman, S. Wolinsky, and N. L. Letvin.** 2004. Immune failure in the absence of profound CD4+ T-lymphocyte depletion in simian immunodeficiency virus-infected rapid progressor macaques. J Virol **78:**275-84.

30. **Ho, D. D., T. R. Rota, R. T. Schooley, J. C. Kaplan, J. D. Allan, J. E. Groopman, L. Resnick, D. Felsenstein, C. A. Andrews, and M. S. Hirsch.** 1985. Isolation of HTLV-III from cerebrospinal fluid and neural tissues of patients with neurologic syndromes related to the acquired immunodeficiency syndrome. N Engl J Med **313:**1493-7.

31. **Holterman, L., H. Niphuis, P. J. ten Haaft, J. Goudsmit, G. Baskin, and J. L. Heeney.** 1999. Specific passage of simian immunodeficiency virus from end-stage disease results in accelerated progression to AIDS in rhesus macaques. J Gen Virol **80** 3089-97.

32. **Katsetos, C. D., J. E. Fincke, A. Legido, H. W. Lischner, J. P. de Chadarevian, E. M. Kaye, C. D. Platsoucas, and E. L. Oleszak.** 1999. Angiocentric CD3(+) T-cell infiltrates in human immunodeficiency virus type 1-associated central nervous system disease in children. Clin Diagn Lab Immunol **6:**105-14.

33. **Kimata, J. T., L. Kuller, D. B. Anderson, P. Dailey, and J. Overbaugh.** 1999. Emerging cytopathic and antigenic simian immunodeficiency virus variants influence AIDS progression. Nat Med **5:**535-41.

34. **Kodama, T., K. Mori, T. Kawahara, D. J. Ringler, and R. C. Desrosiers.** 1993. Analysis of simian immunodeficiency virus sequence variation in tissues of rhesus macaques with simian AIDS. J Virol **67:**6522-34.

35. **Kolchinsky, P., E. Kiprilov, P. Bartley, R. Rubinstein, and J. Sodroski.** 2001. Loss of a single N-linked glycan allows CD4-independent human immunodeficiency virus type 1 infection by altering the position of the gp120 V1/V2 variable loops. J Virol **75:**3435-43.

36. **Kolchinsky, P., T. Mirzabekov, M. Farzan, E. Kiprilov, M. Cayabyab, L. J. Mooney, H. Choe, and J. Sodroski.** 1999. Adaptation of a CCR5-using, primary human immunodeficiency virus type 1 isolate for CD4-independent replication. J Virol **73:**8120-6.

37. **Korber, B.** 2001. Signature and Sequence Variation Analysis. Computational Analysis of HIV Molecular Sequences, p. 55-72 *In* A. G. Rodrigo and G. H. Learn (ed.). Kluwer Academic Publishers, Dordrecht, Netherlands.

38. **Korber, B. T., K. J. Kunstman, B. K. Patterson, M. Furtado, M. M. McEvilly, R. Levy, and S. M. Wolinsky.** 1994. Genetic differences between blood- and brain-derived viral sequences from human immunodeficiency virus type 1-infected patients: evidence of conserved elements in the V3 region of the envelope protein of brain-derived sequences. J Virol **68:**7467-81.

39. **Kuwata, T., H. Dehghani, C. R. Brown, R. Plishka, A. Buckler-White, T. Igarashi, J. Mattapallil, M. Roederer, and V. M. Hirsch.** 2006. Infectious molecular clones from a simian immunodeficiency virus-infected rapid-progressor (RP) macaque: evidence of differential selection of RP-specific envelope mutations in vitro and in vivo. J Virol **80:**1463-75.

40. **Lackner, A. A., S. Dandekar, and M. B. Gardner.** 1991. Neurobiology of simian and feline immunodeficiency virus infections. Brain Pathol **1:**201-12.

41. **Letvin, N. L., M. D. Daniel, P. K. Sehgal, R. C. Desrosiers, R. D. Hunt, L. M. Waldron, J. J. MacKey, D. K. Schmidt, L. V. Chalifoux, and N. W. King.** 1985. Induction of AIDS-like disease in macaque monkeys with T-cell tropic retrovirus STLV-III. Science **230:**71-3.

42. **Letvin, N. L., and N. W. King.** 1990. Immunologic and pathologic manifestations of the infection of rhesus monkeys with simian immunodeficiency virus of macaques. J Acquir Immune Defic Syndr **3:**1023-40.

43. **McArthur, J. C.** 2004. HIV dementia: an evolving disease. J Neuroimmunol **157:**3-10.

44. **McArthur, J. C., N. Haughey, S. Gartner, K. Conant, C. Pardo, A. Nath, and N. Sacktor.** 2003. Human immunodeficiency virus-associated dementia: an evolving disease. J Neurovirol **9:**205-21.

45. **Miller, R. F., P. G. Isaacson, M. Hall-Craggs, S. Lucas, F. Gray, F. Scaravilli, and S. F. An.** 2004. Cerebral CD8+ lymphocytosis in HIV-1 infected patients with immune restoration induced by HAART. Acta Neuropathol (Berl) **108:**17-23.

764 46. **Mori, K., M. Rosenzweig, and R. C. Desrosiers.** 2000. Mechanisms for
765 adaptation of simian immunodeficiency virus to replication in alveolar
766 macrophages. J Virol **74:**10852-9.
767 47. **Morikawa, Y., J. P. Moore, A. J. Wilkinson, and I. M. Jones.** 1991. Reduction
768 in CD4 binding affinity associated with removal of a single glycosylation site in
769 the external glycoprotein of HIV-2. Virology **180:**853-6.
770 48. **Navia, B. A., E. S. Cho, C. K. Petito, and R. W. Price.** 1986. The AIDS
771 dementia complex: II. Neuropathology. Ann Neurol **19:**525-35.
772 49. **Navia, B. A., B. D. Jordan, and R. W. Price.** 1986. The AIDS dementia
773 complex: I. Clinical features. Ann Neurol **19:**517-24.
774 50. **Nei, M., and T. Gojobori.** 1986. Simple methods for estimating the numbers of
775 synonymous and nonsynonymous nucleotide substitutions. Mol Biol Evol **3:**418-
776 26.
777 51. **Novembre, F. J., J. De Rosayro, S. P. O'Neil, D. C. Anderson, S. A. Klumpp,**
778 **and H. M. McClure.** 1998. Isolation and characterization of a neuropathogenic
779 simian immunodeficiency virus derived from a sooty mangabey. J Virol **72:**8841-
780 51.
781 52. **O'Neil, S. P., C. Suwyn, D. C. Anderson, G. Niedziela, J. Bradley, F. J.**
782 **Novembre, J. G. Herndon, and H. M. McClure.** 2004. Correlation of acute
783 humoral response with brain virus burden and survival time in pig-tailed
784 macaques infected with the neurovirulent simian immunodeficiency virus
785 SIVsmmFGb. Am J Pathol **164:**1157-72.

53. **Ohagen, A., A. Devitt, K. J. Kunstman, P. R. Gorry, P. P. Rose, B. Korber, J. Taylor, R. Levy, R. L. Murphy, S. M. Wolinsky, and D. Gabuzda.** 2003. Genetic and functional analysis of full-length human immunodeficiency virus type 1 env genes derived from brain and blood of patients with AIDS. J Virol **77:**12336-45.

54. **Ota, T., and M. Nei.** 1994. Variance and covariances of the numbers of synonymous and nonsynonymous substitutions per site. Mol Biol Evol **11:**613-9.

55. **Pantaleo, G., C. Graziosi, and A. S. Fauci.** 1993. New concepts in the immunopathogenesis of human immunodeficiency virus infection. N Engl J Med **328:**327-35.

56. **Petito, C. K., B. Adkins, M. McCarthy, B. Roberts, and I. Khamis.** 2003. CD4+ and CD8+ cells accumulate in the brains of acquired immunodeficiency syndrome patients with human immunodeficiency virus encephalitis. J Neurovirol **9:**36-44.

57. **Petito, C. K., J. E. Torres-Munoz, F. Zielger, and M. McCarthy.** 2006. Brain CD8+ and cytotoxic T lymphocytes are associated with, and may be specific for, human immunodeficiency virus type 1 encephalitis in patients with acquired immunodeficiency syndrome. J Neurovirol **12:**272-83.

58. **Price, R. W., B. Brew, J. Sidtis, M. Rosenblum, A. C. Scheck, and P. Cleary.** 1988. The brain in AIDS: central nervous system HIV-1 infection and AIDS dementia complex. Science **239:**586-92.

59. **Pumarola-Sune, T., B. A. Navia, C. Cordon-Cardo, E. S. Cho, and R. W. Price.** 1987. HIV antigen in the brains of patients with the AIDS dementia complex. Ann Neurol **21:**490-6.

60. **Ringler, D. J., R. D. Hunt, R. C. Desrosiers, M. D. Daniel, L. V. Chalifoux, and N. W. King.** 1988. Simian immunodeficiency virus-induced meningoencephalitis: natural history and retrospective study. Ann Neurol **23 Suppl:**S101-7.

61. **Roberts, E. S., M. A. Zandonatti, D. D. Watry, L. J. Madden, S. J. Henriksen, M. A. Taffe, and H. S. Fox.** 2003. Induction of pathogenic sets of genes in macrophages and neurons in NeuroAIDS. Am J Pathol **162:**2041-57.

62. **Ryzhova, E. V., P. Crino, L. Shawver, S. V. Westmoreland, A. A. Lackner, and F. Gonzalez-Scarano.** 2002. Simian immunodeficiency virus encephalitis: analysis of envelope sequences from individual brain multinucleated giant cells and tissue samples. Virology **297:**57-67.

63. **Sacktor, N., R. H. Lyles, R. Skolasky, C. Kleeberger, O. A. Selnes, E. N. Miller, J. T. Becker, B. Cohen, and J. C. McArthur.** 2001. HIV-associated neurologic disease incidence changes:: Multicenter AIDS Cohort Study, 1990-1998. Neurology **56:**257-60.

64. **Sharer, L. R., G. B. Baskin, E. S. Cho, M. Murphey-Corb, B. M. Blumberg, and L. G. Epstein.** 1988. Comparison of simian immunodeficiency virus and human immunodeficiency virus encephalitides in the immature host. Ann Neurol **23 Suppl:**S108-12.

65. **Sharer, L. R., E. S. Cho, and L. G. Epstein.** 1985. Multinucleated giant cells and HTLV-III in AIDS encephalopathy. Hum Pathol **16:**760.

66. **Shaw, G. M., M. E. Harper, B. H. Hahn, L. G. Epstein, D. C. Gajdusek, R. W. Price, B. A. Navia, C. K. Petito, C. J. O'Hara, J. E. Groopman, and et al.** 1985. HTLV-III infection in brains of children and adults with AIDS encephalopathy. Science **227:**177-82.

67. **Snider, W. D., D. M. Simpson, S. Nielsen, J. W. Gold, C. E. Metroka, and J. B. Posner.** 1983. Neurological complications of acquired immune deficiency syndrome: analysis of 50 patients. Ann Neurol **14:**403-18.

68. **Tao, B., and P. N. Fultz.** 1995. Molecular and biological analyses of quasispecies during evolution of a virulent simian immunodeficiency virus, SIVsmmPBj14. J Virol **69:**2031-7.

69. **Welch, K., and A. Morse.** 2002. The clinical profile of end-stage AIDS in the era of highly active antiretroviral therapy. AIDS Patient Care STDS **16:**75-81.

70. **Westmoreland, S. V., E. Halpern, and A. A. Lackner.** 1998. Simian immunodeficiency virus encephalitis in rhesus macaques is associated with rapid disease progression. J Neurovirol **4:**260-8.

71. **Williams, K., A. Bar-Or, E. Ulvestad, A. Olivier, J. P. Antel, and V. W. Yong.** 1992. Biology of adult human microglia in culture: comparisons with peripheral blood monocytes and astrocytes. J Neuropathol Exp Neurol **51:**538-49.

72. **Williams, K. C., S. Corey, S. V. Westmoreland, D. Pauley, H. Knight, C. deBakker, X. Alvarez, and A. A. Lackner.** 2001. Perivascular macrophages are the primary cell type productively infected by simian immunodeficiency virus in

the brains of macaques: implications for the neuropathogenesis of AIDS. J Exp Med **193:**905-15.

73. **Zhang, M., B. Gaschen, W. Blay, B. Foley, N. Haigwood, C. Kuiken, and B. Korber.** 2004. Tracking global patterns of N-linked glycosylation site variation in highly variable viral glycoproteins: HIV, SIV, and HCV envelopes and influenza hemagglutinin. Glycobiology **14:**1229-46.

74. **Zink, M. C., A. M. Amedee, J. L. Mankowski, L. Craig, P. Didier, D. L. Carter, A. Munoz, M. Murphey-Corb, and J. E. Clements.** 1997. Pathogenesis of SIV encephalitis. Selection and replication of neurovirulent SIV. Am J Pathol **151:**793-803.

Table 1. Analysis of nonsynonymous to synonymous changes in gp120 at sequential timepoints

	Average dN/dS[a]							
	H631				H636			
week post inoculation	CSF		Plasma		CSF		Plasma	
1	0.043	(9)[b]	0.231	(10)	0.208	(8)	0.156	(9)
32	0.796	(9)	0.696	(9)	1.035	(4)	0.990	(7)
76	1.607	(10)	1.488	(10)	0.821	(10)	1.355	(10)
116 (death)	2.427	(9)	2.746	(9)	NA[c]		NA	

[a] Average ratio of nonsynonymous (dN) to synonymous (dS) change as calculated by SNAP

[b] Number of clones used to determine the average dN/dS ratio

[c] Not applicable

FIGURE LEGENDS

Fig. 1. Viral RNA levels in plasma (A) and CSF (B). Samples were obtained at sequential time points post inoculation. Y axis represents viral RNA load (copies/ml) and the X axis represents weeks post inoculation. Macaques H631 (square symbol) and H636 (circle symbol) are shown in red and the rapid progressor macaque H635 is shown in blue.

Fig. 2. SIV-specific in situ hybridization and immunohistochemistry of infiltrating cell populations in the brain of conventional progressor macaques with SIVE, H631 and H636. Prominent perivascular mononuclear infiltrates stained specifically with antibodies to CD3 (H631), CD8 (H631), and CD20 (H636) on the left identified by DAB substrate (brown). The right panels show the infiltration of macrophages as evident by staining with HAM56 in red (H636), with an inset of a characteristic $HAM56^{+}$ multinucleated giant cell. A serial section shows the expression of SIV RNA in these infiltrating cells in blue. The bottom right panel shows confocal microscopy of the brain of H636 showing that SIV-expressing cells (green), co-expressed HAM56 (white) consistent with their identification as macrophages although uninfected $CD3^{+}$ T cells (red) were also present.

Fig. 3. Sequence analysis of the V1/V2 region of gp120 clones directly from CSF and plasma viral RNA in H631 (A) and H636 (B) obtained from weeks 32 and 76 post inoculation. In addition, samples obtained at week 116 (death) for H631 are shown in (A). Amino acid numbering is based on SIVsmE543-3 sequence. Amino acid

887 substitutions are indicated, dashes indicate deletions, a dot indicates identity, and
888 potential N-linked glycosylation sites are underlined.
889
890 Fig. 4. Evolution of gp120 region isolated from CSF and plasma in H631 (A) and H636
891 (B). Sequential samples were obtained at weeks 1, 32, 76, and 116 (death, H631) post
892 inoculation. The phylogenetic tree was analyzed using the maximum likelihood distance
893 model as described in Materials and Methods and is rooted on SIVsmE543-3 gp120
894 sequence. The scale shows the number of substitutions per site.
895
896 Fig. 5. Representative replication of isolated viruses in donor rhesus PBMC (A and B)
897 and monocyte-derived macrophages (MDM) (C and D). (A) Replication of H631 isolates
898 in PBMC. (B) Replication of H636 isolates in PBMC. (C) Replication of H631 isolates
899 in MDM. (D) Replication of H636 isolates in MDM. SIVsmE543-3 was used as control
900 (shown in gray) and replication was monitored by RT activity of culture supernatants (Y
901 axis). Days post infection are shown along the X axis. Solid black lines represent virus
902 isolated from plasma and solid red lines represent virus isolated from the CNS.
903
904 Fig. 6. Mean replication of isolated viruses in four different rhesus donor PBMC (A and
905 B) and MDM (C and D). Infections in each donor were performed twice Data on graph
906 represent the mean and standard error of the mean are plotted as error bars. All other
907 information is same as defined in Fig. 5 legend.
908

909 Fig.7. Phylogenetic analyses of envelope region from viruses isolated from H631 (A)
910 and H636 (B). Panel C illustrates phylogenetic analysis of envelope obtained directly
911 from CSF and plasma of the rapid progressor H635. The phylogenetic tree was analyzed
912 using the maximum likelihood distance model as described in Materials and Methods and
913 is rooted on SIVsmE543-3 gp160 sequence. The scale shows the number of substitutions
914 per site. Bootstrap support values are based on 1000 replicates. Only values greater than
915 70% at the major nodes are shown.
916
917 Fig. 8. Comparison of the number of potential N-linked glycosylation sites (PNGS) in
918 envelope of the isolated viruses to E543-3. Error bar represents SEM. Asterisk indicates
919 that the loss of PNGS was statistically significant compared to E543-3 by one sample T
920 test, two tailed, *P* values ranged from 0.0001 to 0.0054. Double asterisks indicate that
921 since all nine clones of H636 CSF virus had 24 PNGS, there is no error bar.
922

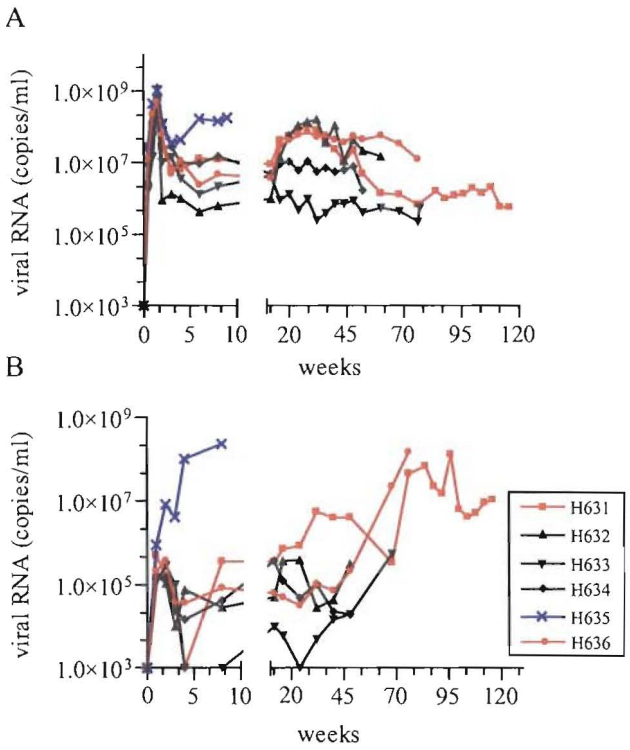
A
viral RNA (copies/ml)
1.0×10^9
1.0×10^7
1.0×10^5
1.0×10^3
0
5
10
20
45
70
95
120
weeks
B
viral RNA (copies/ml)
1.0×10^9
1.0×10^7
1.0×10^5
1.0×10^3
0
5
10
20
45
70
95
120
weeks
H631
H632
H633
H634
H635
H636

Figure 1

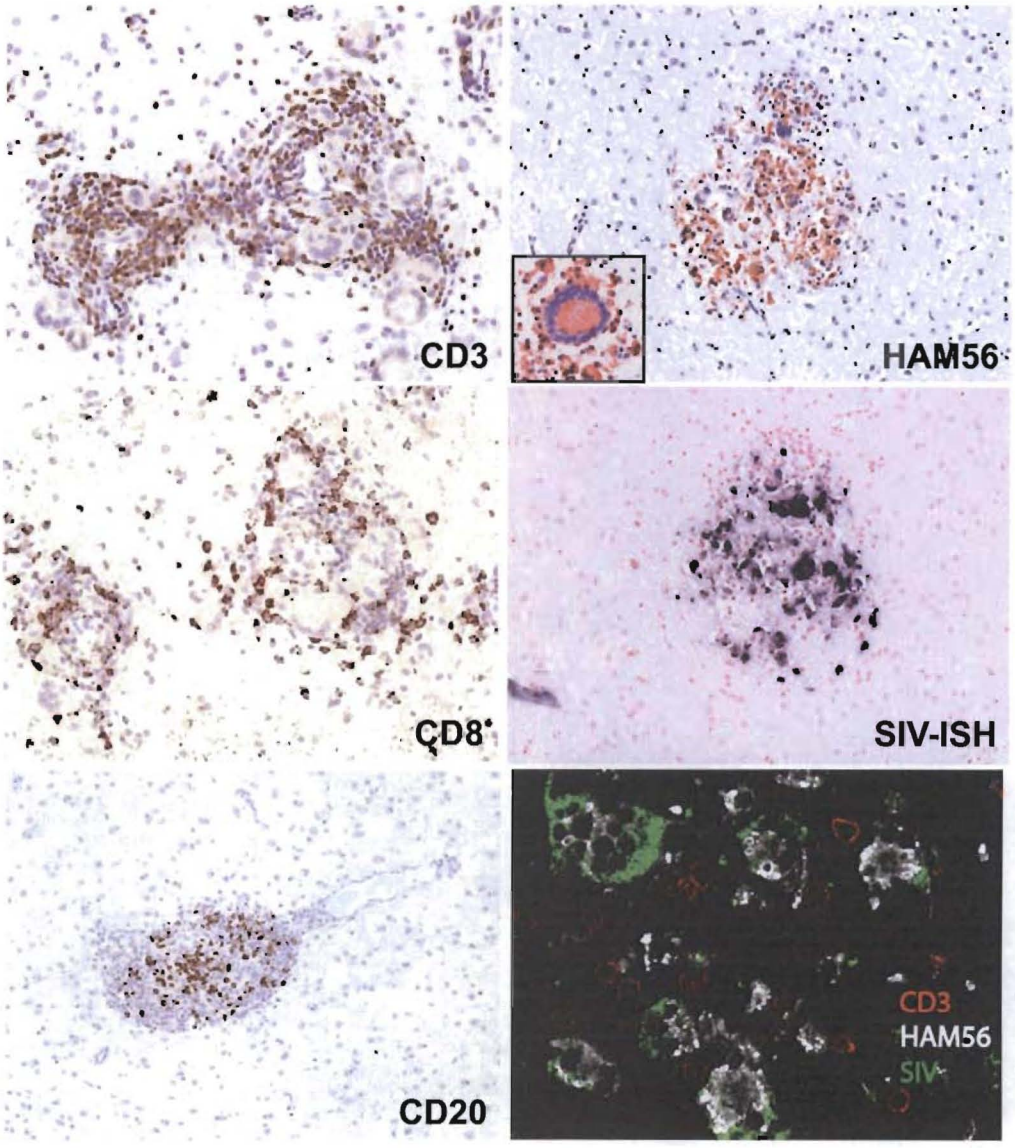

FIGURE 2

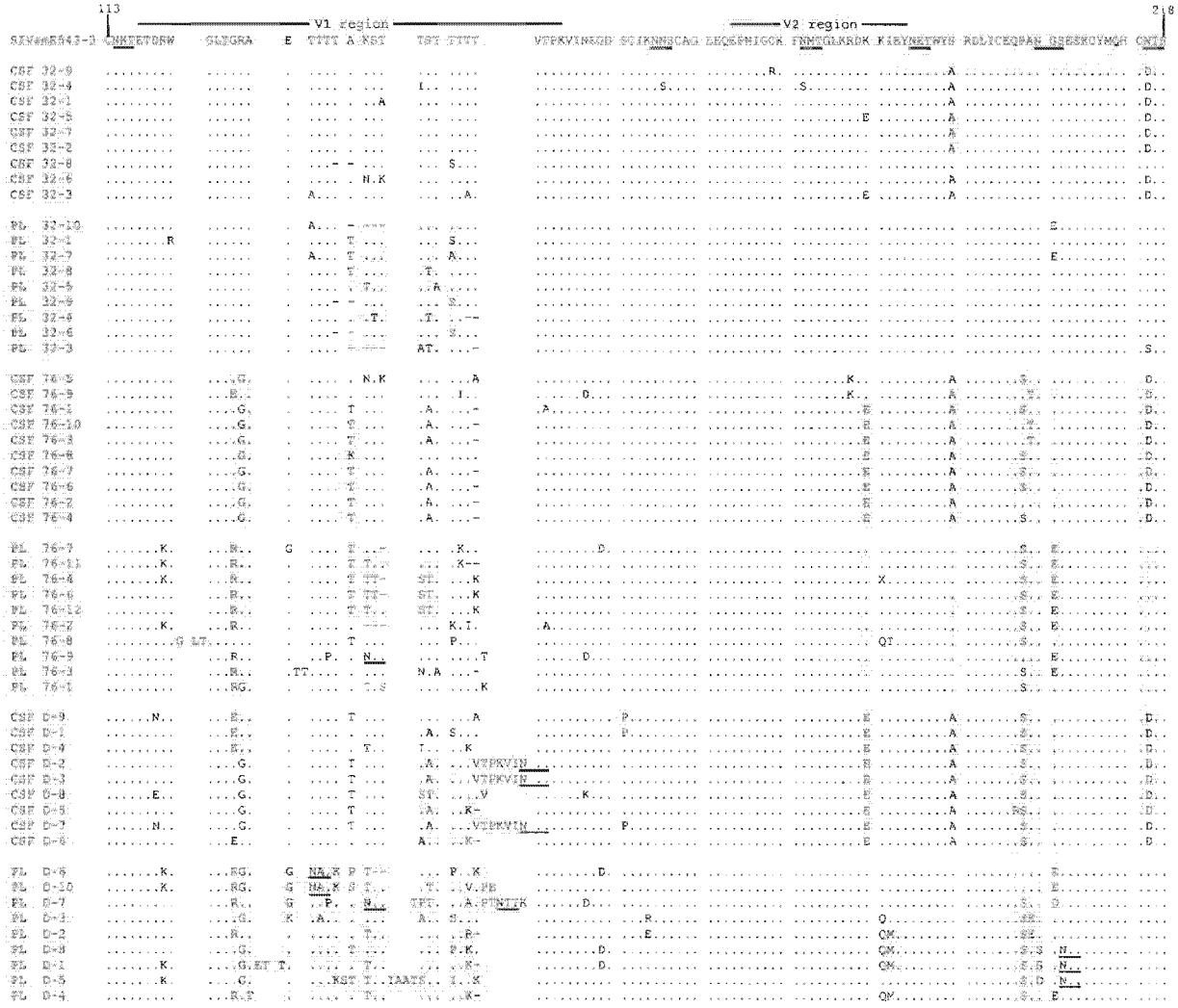

Figure 3A.

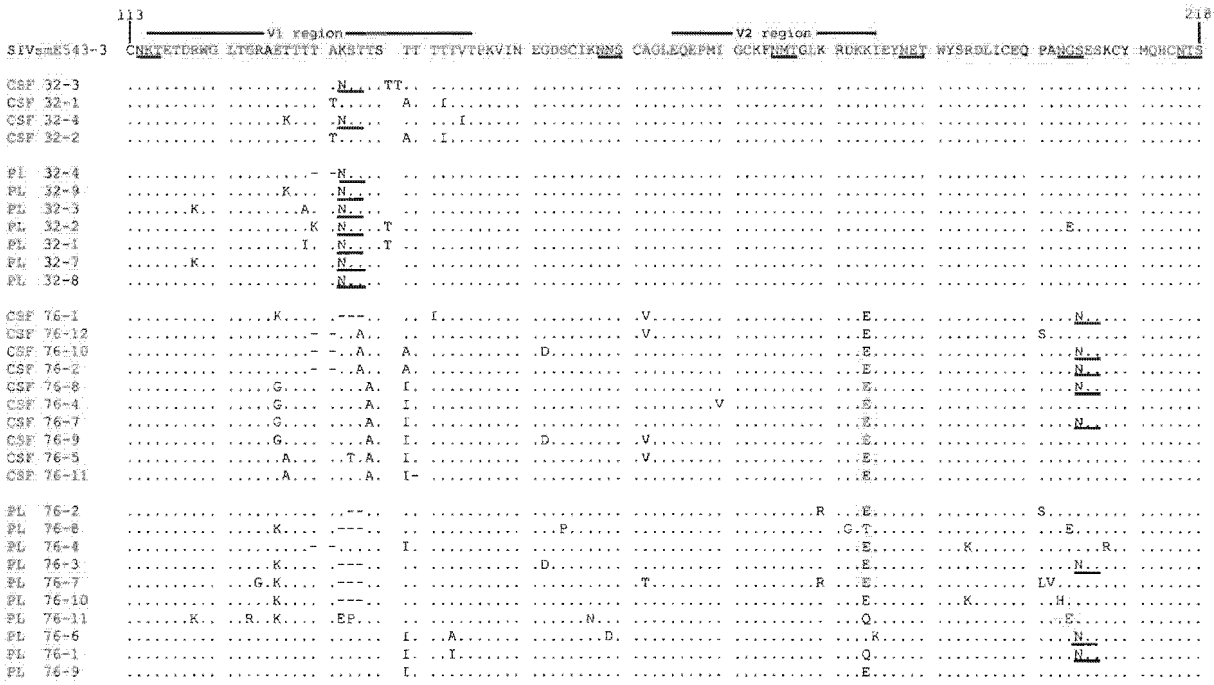
113
V1 region
V2 region
218
SIVsmE543-3 CNKTETDRWG LTGRAETTTT AKSTTS TT TTIVTPKVIN EGDSCIKNNS CAGLEQEPMI GCKFNMTGLK RDKKIEYNET WYSRDLICEQ PANGSESKCY MQHCNTS

Figure 3B

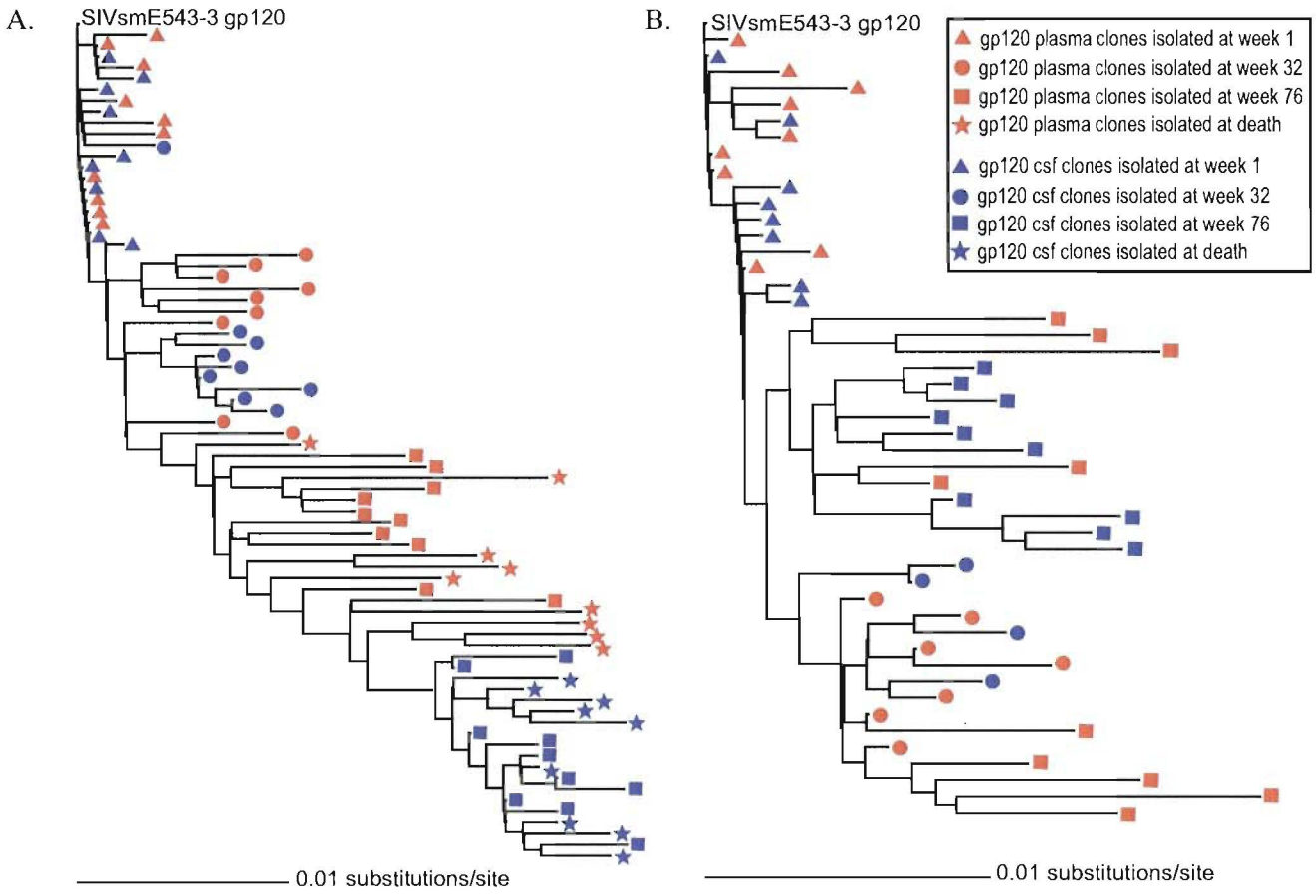
A.
SIVsmE543-3 gp120
0.01 substitutions/site
B.
SIVsmE543-3 gp120
gp120 plasma clones isolated at week 1
gp120 plasma clones isolated at week 32
gp120 plasma clones isolated at week 76
gp120 plasma clones isolated at death
gp120 csf clones isolated at week 1
gp120 csf clones isolated at week 32
gp120 csf clones isolated at week 76
gp120 csf clones isolated at death
0.01 substitutions/site

Figure 4

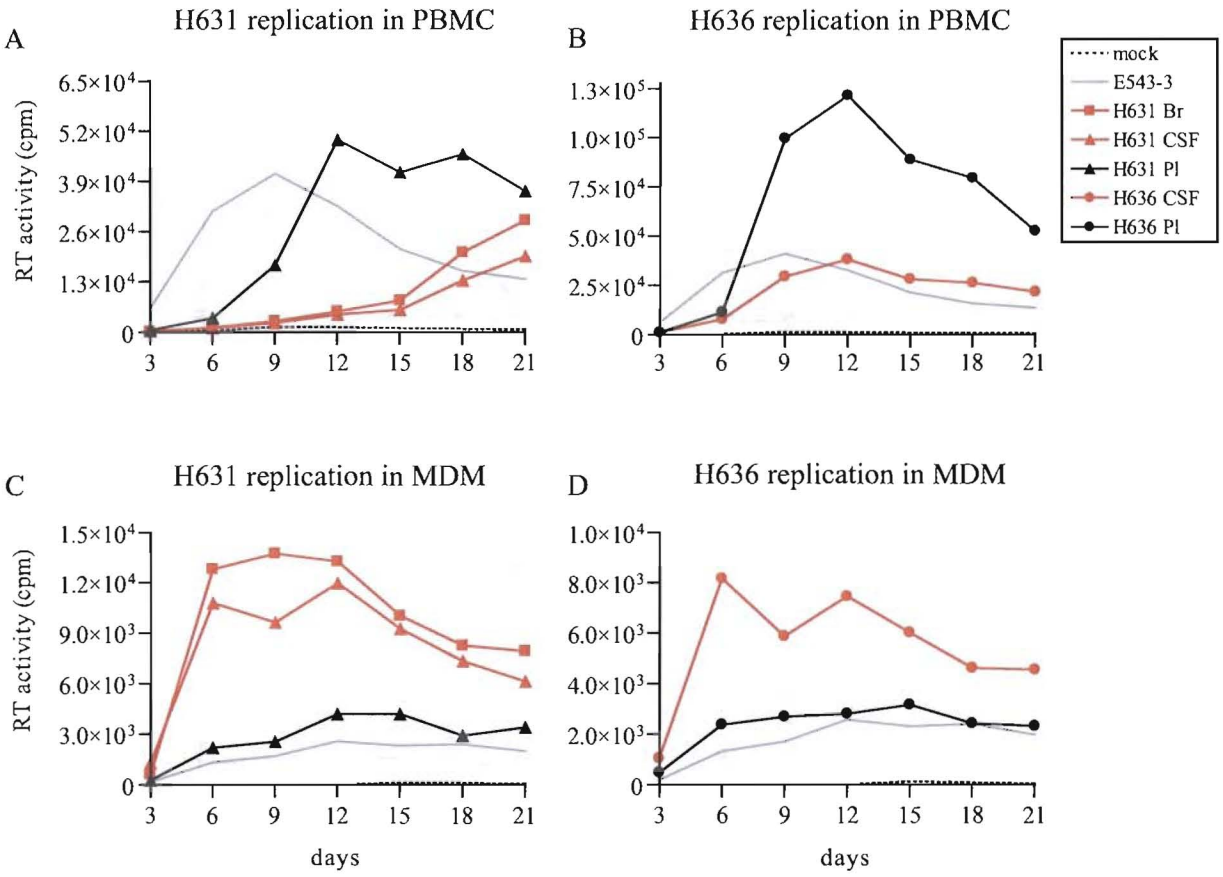
A
H631 replication in PBMC
B
H636 replication in PBMC
mock
E543-3
H631 Br
H631 CSF
H631 Pl
H636 CSF
H636 Pl
RT activity (cpm)
6.5×10⁴
5.2×10⁴
3.9×10⁴
2.6×10⁴
1.3×10⁴
0
1.3×10⁵
1.0×10⁵
7.5×10⁴
5.0×10⁴
2.5×10⁴
3 6 9 12 15 18 21
C
H631 replication in MDM
D
H636 replication in MDM
1.5×10⁴
1.2×10⁴
9.0×10³
6.0×10³
3.0×10³
1.0×10⁴
8.0×10³
6.0×10³
4.0×10³
2.0×10³
days

Figure 5

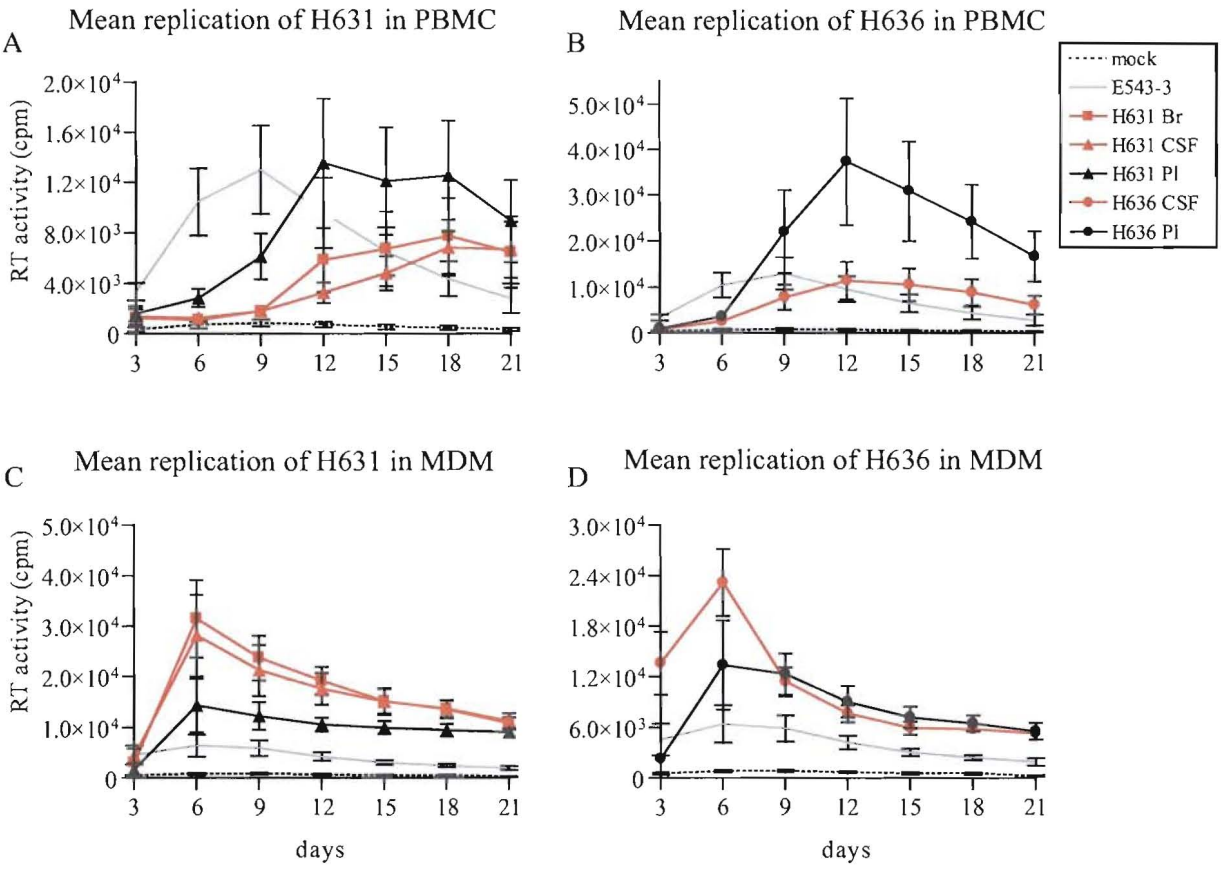
A
Mean replication of H631 in PBMC
B
Mean replication of H636 in PBMC
C
Mean replication of H631 in MDM
D
Mean replication of H636 in MDM
RT activity (cpm)
days
mock
E543-3
H631 Br
H631 CSF
H631 Pl
H636 CSF
H636 Pl

Figure 6

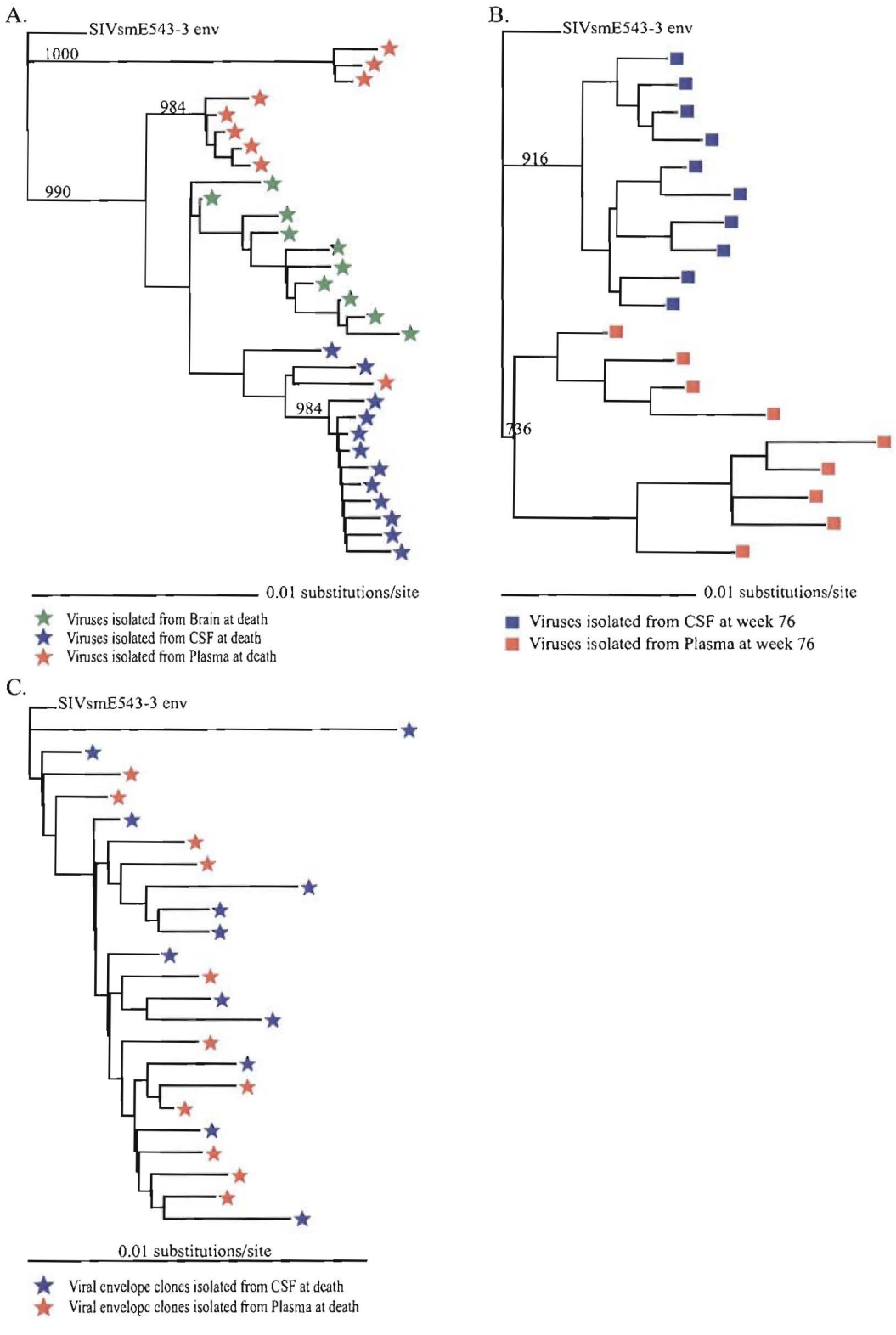
A.
SIVsmE543-3 env
1000
984
990
984
0.01 substitutions/site
Viruses isolated from Brain at death
Viruses isolated from CSF at death
Viruses isolated from Plasma at death
B.
SIVsmE543-3 env
916
736
0.01 substitutions/site
Viruses isolated from CSF at week 76
Viruses isolated from Plasma at week 76
C.
SIVsmE543-3 env
0.01 substitutions/site
Viral envelope clones isolated from CSF at death
Viral envelope clones isolated from Plasma at death

Figure 7

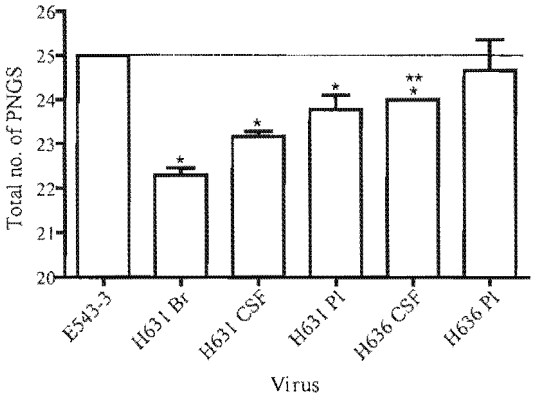

* Statistically significant, P values range from 0.0001 to 0.0054 when compared to E543-3.

** Because all 9 clones had 24 PNGS, there is no error bar.

Figure 8